Evolution of the Voltage Sensor Domain of the Voltage-Sensitive Phosphoinositide Phosphatase VSP/TPTE Suggests a Role as a Proton Channel in Eutherian Mammals

Keith A. Sutton,[1] Melissa K. Jungnickel,[1] Luca Jovine,[2] and Harvey M. Florman*,[1]

[1]Department of Cell Biology, University of Massachusetts Medical School

[2]Department of Biosciences and Nutrition, Center for Biosciences, Karolinska Institutet, Huddinge, Sweden

***Corresponding author:** E-mail: harvey.florman@umassmed.edu.

Associate editor: Willie Swanson

Abstract

The voltage-sensitive phosphoinositide phosphatases provide a mechanism to couple changes in the transmembrane electrical potential to intracellular signal transduction pathways. These proteins share a domain architecture that is conserved in deuterostomes. However, gene duplication events in primates, including humans, give rise to the paralogs TPTE and TPTE2 that retain protein domain organization but, in the case of TPTE, have lost catalytic activity. Here, we present evidence that these human proteins contain a functional voltage sensor, similar to that in nonmammalian orthologs. However, domains of these human proteins can also generate a noninactivating outward current that is not observed in zebra fish or tunicate orthologs. This outward current has the anticipated characteristics of a voltage-sensitive proton current and is due to the appearance of a single histidine residue in the S4 transmembrane segment of the voltage sensor. Histidine is observed at this position only during the eutherian radiation. Domains from both human paralogs generate proton currents. This apparent gain of proton channel function during the evolution of the TPTE protein family may account for the conservation of voltage sensor domains despite the loss of phosphatase activity in some human paralogs.

Key words: voltage sensor domain, proton channel, ion channel, phosphoinositide phosphatase, sperm.

Research article

Introduction

The voltage-sensitive phosphatase (VSP) proteins are a family of phosphoinositide phosphatases. Principal substrates for this enzyme include phosphatidylinositol-4,5-diphosphate and phosphatidylinositol-3,4,5-trisphosphate (Iwasaki et al. 2008; Halaszovich et al. 2009). By controlling the levels of these phospholipids, VSP may regulate signal transduction through both phospholipase C- and 1-phosphatidylinositol-3-kinase pathways (Balla 2006) as well as the activity of a number of ion channels (Suh and Hille 2008).

A signature feature of VSP proteins is the presence of a voltage sensor domain. Cells maintain an electrical potential across membranes at considerable metabolic cost and use it to control a number of vital processes (Laughlin et al. 1998). Changes in this potential are detected by specialized sensor domains, the best studied of which is a module, conserved from archaea to mammals, that is composed of four transmembrane segments (S1–S4). Basic residues in the S4 segment, as well as charged residues in other transmembrane regions, move in response to shifts in the electrical potential and control effector domains (Okamura 2007; Swartz 2008). This voltage sensor domain was identified first in voltage-sensitive cation channels (Noda et al. 1986), where sensor movements control the ion permeability through an adjacent permeability pore domain and underlie the regulation of classical K^+, Na^+, and Ca^+ channels (Hille 2001; Swartz 2008). In the VSP family, the sensor is instead coupled to a phosphatase catalytic domain and regulates enzymatic activity (Murata et al. 2005; Okamura et al. 2009).

This lipid phosphatase family is conserved in deuterostomes. VSP was first identified as a flagellar plasma membrane protein in sperm of the sea squirt, *Ciona intestinalis* (Murata et al. 2005), and transcripts were later detected in other tissues of that tunicate (Ogasawara et al. 2011). Mammalian orthologs include TPTE (*T*ransmembrane *P*hosphatase with *Te*nsin Homology), which is highly expressed in the spermatogenic lineage (Chen et al. 1999; Guipponi et al. 2001; Wu et al. 2001; Tapparel et al. 2003), within the embryonic nervous system (Reymond et al. 2002), and in a variety of tumors (Sjoblom et al. 2006; Jones et al. 2008; Parsons et al. 2008, 2011; Pleasance et al. 2010). In addition, a paralog, TPTE2, is present in primates, including humans, and is expressed in spermatogenic cells and a limited number of other tissues (Walker et al. 2001).

However, little is known about the function of mammalian orthologs. First, catalytic activity of VSP from *C. intestinalis*, the zebra fish *Danio rerio*, and the amphibians *Xenopus laevis* and *X. tropicalis* is regulated by membrane potential (Murata et al. 2005; Worby and Dixon 2005; Murata and Okamura 2007; Hossain et al. 2008; Ratzan et al. 2011). Bioinformatic analysis suggests that mammalian orthologs may also contain a voltage sensor domain (Kumanovics et al. 2002), but it has not been shown that this domain is functional. Second, the site of action of these

proteins in mammals is not known. VSP of *C. intestinalis* has been reported to be a sperm plasma membrane protein, and zebra fish and *Xenopus* orthologs traffic to the plasma membrane in heterologous expression systems (Hossain et al. 2008; Ratzan et al. 2011). In contrast, mammalian orthologs appear to be restricted to the Golgi complex, both in spermatogenic cells and following expression in cell lines (Guipponi et al. 2001; Walker et al. 2001; Wu et al. 2001). Finally, the nonmammalian VSP proteins that have been examined are all catalytically active (Murata et al. 2005; Hossain et al. 2008; Ratzan et al. 2011). In contrast, the paralogous proteins in primates are highly conserved, but TPTE2 has phosphatase activity while sequence variations in primate TPTE resulted in a loss of catalytic activity (Walker et al. 2001; Leslie et al. 2007).

In order to resolve some of these uncertainties, we set out to determine whether the voltage sensor domains of mammalian TPTE and TPTE2 were functional. Here, we report human (Hs-) TPTE or TPTE2 sequences, when introduced into the zebra fish VSP, exhibit currents reflective of sensor activation. In addition, these human sequences produce a voltage-sensitive proton current. Proton channel activity was conserved between Hs-TPTE and Hs-TPTE2 and so may account for the conservation of the voltage sensor domain in primates despite the loss of catalytic activity in some paralogs. This activity is due to the introduction of a single histidine residue that first appears in the S4 segment of TPTE during the radiation of eutherian mammals.

Materials and Methods

DNA Methods

cDNA for Dr-VSP (IRBV clone 7167382) and Hs-TPTE (IRAT clone 5269598) was obtained from Open Biosystems. Amino acid positions for Hs-TPTE and Hs-TPTE2 were based on the longest isoforms (TPTEα, GI: 109689707; TPTE2γ, GI: 213972591). Mutagenesis was carried out with a QuikChange kit (Stratagene), and HEK293 cells were transfected with Effectene (QIAGEN).

Structural Modeling and Alignments

A 3D model of the voltage sensor domain of Hs-TPTE (amino acid residues 71–221 of NP_954870.2) was obtained by homology modeling with YASARA Structure (Krieger et al. 2009), based on the X-ray structures of the S1–S4 region of the Shaker family potassium channel (PDB ID 2R9R, Long et al. 2007), Kv2.1 paddle-Kv1.2 chimera (PDB ID 3LNM, Tao et al. 2010), and NavAb voltage-gated Na^+ channel (PDB ID 3RVY and 3RW0, Payandeh et al. 2011). After refinement by molecular dynamics simulation in water (Krieger et al. 2004; Chetwynd et al. 2008), the final model had a YASARA quality score of 0.17. Similar regions in orthologous proteins were identified using eggNOG 2.0 (http://eggnog.embl.de; Muller et al. 2010).

Evolutionary Analysis

The following Ensembl transcripts were used for analysis of positive selection: Chimpanzee ENSPTRT00000010459, Gorilla ENSGGOT00000001624, Orangutan ENSPPYT00000006133, Marmoset ENSCJAT00000034679, Gibbon ENSNLET00000017408, Macaque ENSMMUT00000010321, Bush baby ENSOGAT00000027619, Panda ENSAMEG00000011739, Cow ENSBTAT00000035777, Dog ENSCAFT00000009601, Elephant ENSLAFT00000026716, Horse ENSECAT00000008826, Microbat ENSMLUT00000030189, Sloth ENSCHOT00000000485, Pig ENSSSCT00000010271, Rabbit ENSOCUT00000025349, Rat ENSRNOT00000034670, Mouse ENSMUST00000077194, Kangaroo rat ENSDORT00000014380, and Platypus ENSOANT00000024445. Human transcripts were not included due to the presence of two genes (TPTE and TPTE2) and the presence of numerous pseudogenes. A region of TPTE corresponding to nucleotide positions 730–1383 of the mouse sequence was used. Alignment was initially performed using MegAlign (Lasergene 9, DNASTAR) and manually validated. Sequence analysis was performed using the Datamonkey (http://www.datamonkey.org/; Pond and Frost 2005) implementation of the HyPhy package of analysis tools (Pond et al. 2005). This test revealed no evidence of positive selection at the position of histidine-207 of human TPTE.

Electrophysiological Methods

Currents were recorded from HEK293 cells at room temperature using an external solution containing N-methyl-D-glucamine (75 mM), HEPES (80 mM), $CaCl_2$ (1 mM), $MgCl_2$ (1 mM), and glucose (10 mM) and an internal solution of N-methyl-D-glucamine (65 mM), $MgCl_2$ (3 mM), ethylene glycol tetraacetic acid (1 mM), and HEPES (100 mM). pH was adjusted with methanesulfonic acid. NaCl was added by substitution with N-methyl-D-glucamine$^+$-sulfonate$^-$. Whole-cell currents were acquired using Clampex 9.0 (Axon Instruments), filtered at 2 kHz, and leak components were subtracted using a $p/n = 5$ protocol. Proton currents were measured at the end of the depolarizing test pulse.

Charge–voltage (Q-V) relationships for the activation and inactivation of Dr-VSP gating currents were fit by the Boltzmann equation ($Q = 1/(\exp(ze(V-V_{1/2})kT))$), where z is the valance, e is the elementary electric charge, V and $V_{1/2}$ are membrane voltage and the voltage for a half-maximal response, k is Boltzmann's constant, and T is absolute temperature. Fitting was carried out using OriginPro 8.5 (OriginLab, Northampton MA) and used to calculate $V_{1/2}$.

Results

Evidence That Domains of Human TPTE and TPTE2 Move in Response to Membrane Depolarization

There are two identified activities of voltage sensor domains: the sensor moves in response to changes in membrane potential and sensor movement activates targets. Since Hs-TPTE lacks catalytic activity, we instead examined sensor movements. Those movements result in a translocation of charged residues in transmembrane segments of the sensor and so generate a "sensing current" that is a signature of a functional voltage sensor (Armstrong and

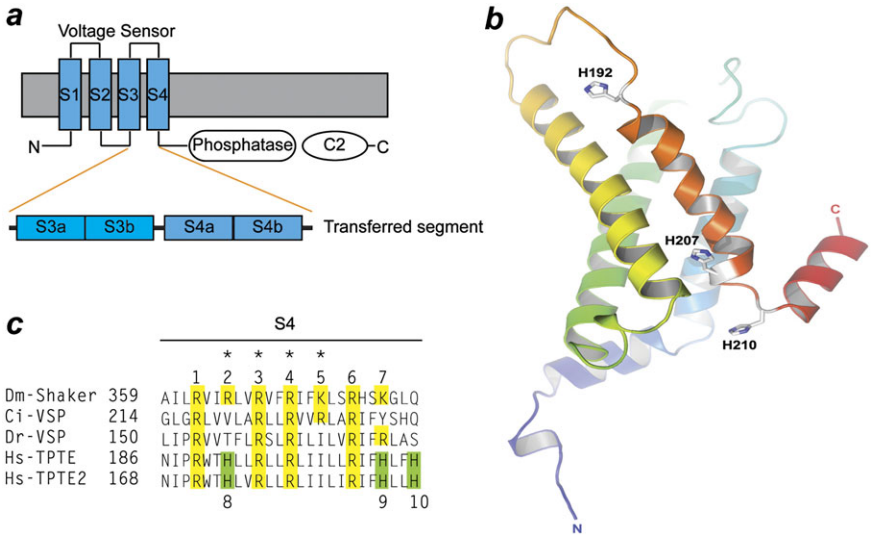

Fig. 1. Domain structure of VSP/TPTE proteins. (*a*) Members of the VSP/TPTE family contain a voltage sensor consisting of four transmembrane segments (S1–S4), followed by a phosphoinositide phosphatase domain and a C2 region. Intracellular and extracellular regions are based on the orientation of Shaker Kv channels. The paddle motif is identified in structural studies and consists of the S3b and S4a portions of the voltage sensor. Domain swapping experiments used the S3-loop-S4 segment. (*b*) A homology model of the Hs-TPTE voltage sensor, constructed on the basis of the Shaker K^+ channel, the Kv2.1 paddle-Kv1.2 chimera, and the NavAb voltage-gated Na^+ channel, was used to identify transmembrane segments (S1, blue; S2, green; S3, yellow; and S4 orange). The three histidine residues present in and near the S4 segment of Hs-TPTE but not present in non-eutherian VSP are shown in stick representation (numbering based on Hs-TPTE, GI: 109689707). This figure and supplementary figure 2 (Supplementary Material online) were made with PyMOL (The PyMOL Molecular Graphics System, Version 1.4.1; Schrödinger, LLC). (*c*) Alignment of S4 segments shows that the positions of basic residues (shaded in yellow) in VSP/TPTE family members and in a Shaker Kv channel are conserved (numbered 1–7 based on Shaker sequence). Sequences include: *Drosophila melanogaster* Dm-Shaker Kv (GI: 288442), *Ciona intestinalis* Ci-VSP (GI: 66391023), *Danio rerio* Dr-VSP (GI: 193248592), *Homo sapiens* Hs-TPTE (GI: 109689707), and Hs-TPTE2 (GI: 213972591). The positions of three histidine residues present in human TPTE/TPTE2 are indicated (shaded in green, numbered 8–10). Asterisks indicate arginine residues of Dm-Shaker Kv that yield proton currents when mutated to histidine (Starace et al. 1997; Starace and Bezanilla 2001).

Bezanilla 1973; Bezanilla 2008; Swartz 2008). Sensing currents can be detected in whole-cell patch-clamp experiments.

We set out to detect sensing currents following expression of Hs-TPTE and Hs-TPTE2 in HEK293 cells. However, these proteins do not reach the plasma membrane, consistent with previous reports that Hs-TPTE may be a Golgi complex protein in human spermatogenic cells (Guipponi et al. 2001; Tapparel et al. 2003) and that both human and mouse TPTE localize in the Golgi complex in heterologous expression systems (Guipponi et al. 2001; Walker et al. 2001; Wu et al. 2001; Tapparel et al. 2003). This may reflect the cellular localization of TPTE/TPTE2 in vivo or may be another case in which plasma membrane proteins that are highly expressed in the mammalian spermatogenic lineage (Walker et al. 2001; Wu et al. 2001) fail to reach the cell surface following heterologous expression (Ren et al. 2001; Wang et al. 2003). In contrast, the zebra fish ortholog, Dr-VSP, is trafficked to the plasma membrane efficiently in cell lines (Hossain et al. 2008). In addition, the paddle motif, a helix-loop-helix structure that consists of the S3b and S4a segments of the voltage sensor domain (fig. 1*a*) and that contains determinants of voltage response characteristics during sensor activation (Jiang et al. 2003), is portable and can be transferred between sensors of different proteins (Alabi et al. 2007). This permitted us to use Dr-VSP as a template for the analysis of Hs-TPTE/TPTE2 voltage sensor behavior following transfer of human TPTE/TPTE2 sequences comprising the paddle segment plus flanking regions.

The voltage sensor domains of VSP and of mammalian TPTE are related to those of K^+ and Na^+ channels (Kumanovics et al. 2002; Worby and Dixon 2005; Okamura 2007). Homology modeling demonstrated a good fit of the Hs-TPTE sequence with the X-ray structure of a rat Shaker family Kv channel and with a bacterial Na^+ channel (see Materials and Methods: Structural Modeling and Alignments), thereby allowing the identification of the S3-loop-S4 segment of Hs-TPTE (fig. 1*b*). Multiple sequence alignments were then carried out using eggNOG 2.0 (Muller et al. 2010) to identify related sequences in other orthologs (fig. 1*c*).

Dr-VSP produced transient asymmetric currents following membrane depolarization of HEK293 cells (fig. 2*a* and *b*) that are similar in charge–voltage relationship for activation (ON sensing current calculated $V_{1/2}$, 99.7 ± 2.3 mV; $n = 8$) and inactivation (OFF sensing current $V_{1/2}$, 90.4 ± 3.9 mV; $n = 8$) to the sensing currents observed previously with Dr-VSP (Hossain et al. 2008). These currents were not detected in untransfected cells. We next replaced the S3-loop-S4 region of Dr-VSP with the corresponding region of Hs-TPTE (residues 173–213, designated Dr-VSP$^{HsTPTE:173-213}$) or of TPTE2 (residues 155–195, designated Dr-VSP$^{HsTPTE2:155-195}$). These regions contain the sensor paddle domain as well

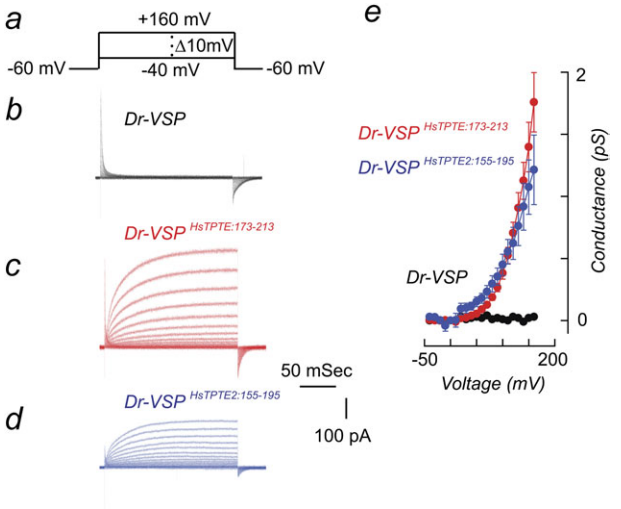

Fig. 2. Properties of the currents generated by Hs-TPTE/TPTE2 domains. Whole-cell patch-clamp currents were recorded from HEK293 cells transfected with Dr-VSP or with Dr-VSP chimeras following transplant of the S3-loop-S4 domains (yellow and orange helices, fig. 1*b*) from Hs-TPTE (Dr-VSP$^{HsTPTE:173-213}$) or from Hs-TPTE2 (Dr-VSP$^{HsTPTE2:155-195}$). (*a*) Voltage protocol used to elicit currents. (*b–d*) Currents recorded in HEK293 cells transfected with (*b*) Dr-VSP (black traces), (*c*) Dr-VSP$^{HsTPTE:173-213}$ (red traces), and (*d*) Dr-VSP$^{HsTPTE2:155-195}$ (blue traces). Transient sensing currents were recorded during depolarization and repolarization steps. Secondary currents were detected in Dr-VSP$^{HsTPTE:173-213}$ and Dr-VSP$^{HsTPTE2:155-195}$ transfectants but not in cells transfected with Dr-VSP. Time and current scales are shown. (*e*) Conductance–voltage relationship for secondary currents of Dr-VSP (black), Dr-VSP$^{HsTPTE:173-213}$ (red), and Dr-VSP$^{HsTPTE2:155-195}$ (blue) are shown. Data represents the mean (±standard error of the mean) of 8–16 independent experiments.

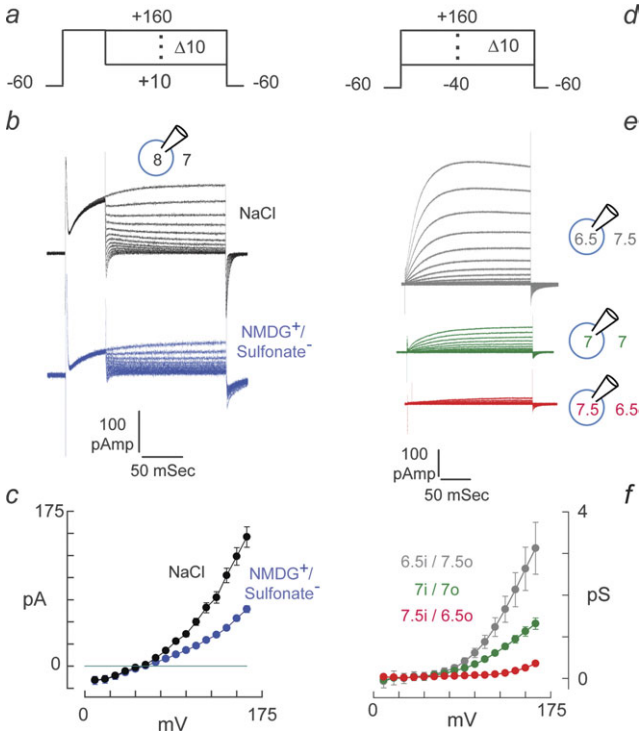

Fig. 3. Secondary currents are due to proton conductance. Whole-cell patch-clamp experiments were carried out on HEK293 cells transfected with Dr-VSP$^{HsTPTE:173-213}$. (*a–c*) Reversal potential was determined using identical intracellular and extracellular ionic conditions except for a 1 pH unit gradient (pH values shown in inset figure of patch-clamped cell). (*a*) Voltage protocol. (*b*) Currents recorded using intracellular and extracellular NaCl solutions (black traces) and with replacement of NaCl with impermeant $NMDG^+$/sulfonate$^-$ solutions (blue traces). (*c*) Current–voltage relationships for cells in NaCl (black line) and $NMDG^+$/sulfonate$^-$ (blue line) media, based on traces shown in *b*. Solid horizontal line indicates zero conductance. (*d–f*) The effects of pH gradient on secondary current amplitude. (*d*) Voltage protocol. (*e*) Current traces were recorded under symmetrical ionic conditions except for the indicated pH gradients (pH values shown in inset figure of patch-clamped cells). (*f*) Conductance–voltage relationship as a function of pH gradient (6.5 in/7.5 out, gray; 7.0 in/7.0 out, green; and 7.5 in/6.5 out, red) based on traces shown in *e*. Data (*c*, *f*) represent the mean (±standard error of the mean) of 7–12 independent experiments.

as flanking sequences (fig. 1*a*). Transient asymmetric currents that were similar to the sensing currents of Dr-VSP were also observed following depolarization of cells expressing either chimeric protein. These results, taken together with bioinformatics identification of a sensor domain in TPTE (Kumanovics et al. 2002), strongly suggest that this domain is functional and moves in response to shifts in membrane potential.

However, this sensing current in chimeric proteins was followed by an unanticipated secondary current that is not seen in Dr-VSP transfectants (current montages, fig. 2*b*—Dr-VSP, traces shown in black; fig. 2*c* and *d*—TPTE and TPTE2 chimera, data are shown in red and blue, respectively; fig. 2*e*, summary conductance–voltage relationships) or reported previously for either zebra fish or sea squirt VSP (Murata et al. 2005; Hossain et al. 2008). Detailed analysis of voltage sensor movements will be reported separately. Here, we focus on the nature of this secondary current and its evolutionary implications.

Secondary Currents Are Due to a Voltage-Sensitive Proton Current Activity

Secondary currents generated by chimeric proteins are voltage dependent, outwardly rectifying (current–conductance relationships, fig. 2*e*; TPTE and TPTE2 chimera data are shown in red and blue, respectively) and detected only at membrane potentials that were sufficient to generate sensing currents (supplementary fig. S1, Supplementary Material online). A similar result was obtained when the S4 segment of Dr-VSP was "humanized" by multiple point mutations rather than by domain exchange.

Secondary currents were observed initially when cells expressing chimeric proteins were bathed in complete Ringer's solution (current traces in black, fig. 3*a*; current–voltage relationship in black, fig. 3*c*). However, these currents persisted when the contribution of endogenous channels was minimized by using intracellular and extracellular solutions in which the major physiological salts were replaced by compounds that dissociate into large ions that are not readily conducted by voltage-gated

channels (current traces and current–voltage relationship in blue, fig. 3*b* and *c*).

The persistence of secondary currents in media depleted of the major physiological ions suggested that this current may be due to proton transport. Four other observations are consistent with this. First, the reversal potential of secondary currents in media with a transmembrane pH gradient, but otherwise, symmetrical intracellular/extracellular media that were depleted of the major permeant ions (by replacement of anions and cations in Ringer's solution with $NMDG^+$-$sulfonate^-$), was 58.6 + 2.1 mV ($n = 7$; fig. 3*c*) for a 1 pH unit gradient and 87.5 ± 1.8 ($n = 6$) for a 1.5 pH unit gradient, as predicted by the Nernst equation with protons as a charge carrier. This reversal potential in the presence of a 1 pH unit gradient was not altered when $NMDG^+$-$sulfonate^-$ was replaced by 50 mM NaCl in both intracellular and extracellular solutions (61.8 ± 8.1 mV, $n = 5$; fig. 3*c*). This suggests that Na^+ and Cl^- are not required for secondary current. Third, amplitude of secondary current increased as the outwardly directed proton concentration gradient increased (fig. 3*d–f*). Finally, the $V_{1/2}$ for secondary current shifts with changes in the transmembrane pH gradient (fig. 3*f*), as expected for voltage-sensitive proton currents.

The secondary current generated by Dr-VSP chimera was similar to the proton current produced by HVCN1 channels in its slowly developing time course, outward rectification, and lack of requirement for physiological salts but differed in being ~50-fold less sensitive to inhibition by extracellular Zn^{2+}; 100 μM Zn^{2+} produced a 50.5 ± 0.1% block ($n = 3$) of the Dr-VSP$^{HsTPTE:173-213}$ proton current, whereas that cation inhibited HVCN1 proton currents with an IC_{50} of ~2 μM (DeCoursey and Cherny 2007; Ramsey et al. 2010). This was anticipated as Dr-VSP$^{HsTPTE:173-213}$ lacks a key residue required for a high affinity Zn^{2+} block of HVCN1 (Ramsey et al. 2006) and demonstrated that the proton currents generated by these chimeric proteins were not due to the activation of an endogenous HVCN1 in HEK293 cells.

Molecular Basis of Proton Currents

Transfer of a 40 amino acid sequence, corresponding to the S3-loop-S4 segment of the voltage sensor, from Hs-TPTE/TPTE2 to Dr-VSP results in the production of a novel secondary current. This sequence includes the paddle domain (Jiang et al. 2003) and several flanking residues (fig. 1*a*). In comparing voltage sensor sequences in VSP/TPTE orthologs, we noted histidine residues in or near the S4 segment of Hs-TPTE and of Hs-TPTE2 that were not present in VSP from zebra fish or sea squirt (shown as green-shaded residues and numbered 8–10; fig. 1*c*). Mutation of Dr-VSP arginine-171 to histidine (H9, fig. 1*c*; corresponds to histidine 207 of Hs-TPTE) was sufficient to produce voltage-sensitive proton currents that were similar in activation kinetics, voltage dependence, and current amplitude to those generated when the complete S3-loop-S4 region was transferred (fig. 4). Modeling studies indicate that it is unlikely that the effect of this point mutation was due to disruption of the structure of the voltage sensor

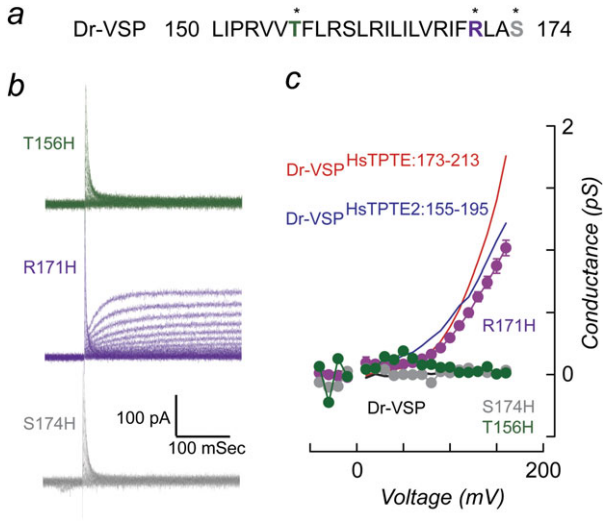

Fig. 4. Proton currents are due to a single histidine in TPTE/TPTE2. (*a*) Sequence of the S4 segment of Dr-VSP is shown, with positions in which histidine is present in Hs-TPTE/TPTE2 indicated (asterisks). (*b*) Current traces for Dr-VSP point mutations. The voltage protocol used to elicit currents was identical to that of figure 2*a*. R171H point mutation of Dr-VSP (purple traces) produced proton currents, whereas T156H (green traces) and S174H (gray traces) mutations failed to conduct currents. (*c*) Conductance–voltage relationship for point mutations of Dr-VSP: T156H (green circles), R171H (purple circles), and S174H (gray circles). Conductances of Dr-VSP (black dashed lines, obscured by gray circles), Dr-VSP$^{HsTPTE:173-213}$ (red line), and Dr-VSP$^{HsTPTE2:155-195}$ (blue line) are shown for comparison (redrawn from fig. 2*e*). Data represent the mean (±standard error of the mean) of 7–12 independent experiments.

(supplementary fig. S2, Supplementary Material online). Conversely, mutation of this conducting histidine of Dr-VSP$^{HsTPTE:173-213}$ to glutamine abrogated this current (fig. 5). This residue is expected to lie near the lipid/cytoplasmic boundary of the S4 segment (fig. 1*b*), based on the X-ray structure of the sensor domain of Kv1.2 channels (Jiang et al. 2003; Long et al. 2007).

In contrast, Dr-VSP did not generate proton currents following point mutation of either threonine-156 or serine-174 to the histidinyl residues found at the corresponding positions of Hs-TPTE and Hs-TPTE2 (data shown in fig. 4; positions of histidines H8 and H10 shown in figs. 1*c* and 4). No other naturally occurring sequence difference between Dr-VSP and Hs-TPTE/TPTE2 produced proton currents in Dr-VSP. We did observe another mutation of Dr-VSP to histidine (arginine168→histidine) that also produced a voltage-sensitive proton current (supplementary fig. S3, Supplementary Material online), but this does not represent a naturally occurring sequence change that has arisen during evolution of the voltage sensor.

Discussion

This study focuses on sequence changes that occur in and near the S4 segment of VSP/TPTE phosphatases during the evolutionary history of these proteins. The positions of positively charged residues in the S4 segment that account for

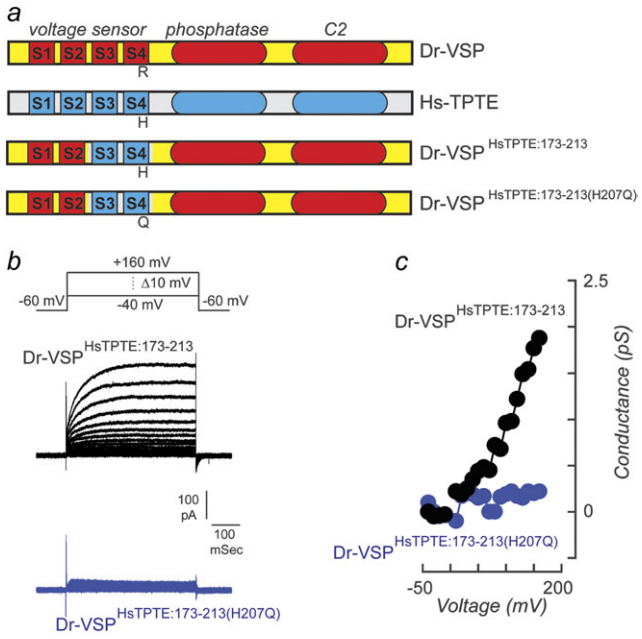

Fig. 5. Role of histidine in the generation of voltage-sensitive proton currents. The proton current conducted by Dr-VSP$^{HsTPTE:173-213}$ is abrogated by mutation of histidine H207 of Hs-TPTE, as shown here for the case of an H207Q mutation of Hs-TPTE:173-213. (*a*) Domain structure of Dr-VSP, Hs-TPTE, and chimeric constructs. Color code: zebra fish domains, red; zebra fish interdomain sequences, yellow; human domains, blue; and human interdomain sequences, gray. Residues corresponding to position 171 of Dr-VSP shown as: Dr-VSP, R171; Hs-TPTE, H207; Dr-VSP$^{HsTPTE:173-213}$, H171; Dr-VSP$^{HsTPTE:173-213(H207Q)}$, H207Q mutation of human sequence. (*b*) HEK293 cells transfected with Dr-VSP$^{HsTPTE:173-213}$ exhibit asymmetric sensing currents (as in fig. 2 in the main text) followed by a secondary current attributed to proton conductance (black traces). However, secondary currents were not observed in cells expressing Dr-VSP$^{HsTPTE:173-213(H207Q)}$ (blue traces). (*c*) Voltage–conductance relationship of currents in HEK293 cells transfected with Dr-VSP$^{HsTPTE:173-213}$ (black) or with Dr-VSP$^{HsTPTE:173-213(H207Q)}$ (blue). Data represent the means (±standard error of the mean, error bars are obscured by the symbols) of five separate experiments.

voltage sensor function are conserved to a great extent within the VSP/TPTE family as well as between VSP/TPTE and corresponding segments of K^+ channels and other cation channels (Worby and Dixon 2005; Okamura 2007). Yet, we noted sequence differences between human (Hs-TPTE and Hs-TPTE2) and zebra fish (Dr-VSP) members of the VSP/TPTE family, particularly regarding the introduction of one histidine residue in the S4 segment of human orthologs and two others that lie just outside S4. One of these histidines (Histidine-207 of Hs-TPTE; shown as H9 in fig. 1*c*), when present in the context of Dr-VSP, converted that zebra fish protein into a voltage-gated proton current.

The VSP/TPTE family is conserved from ascidians to mammals. However, inspection of available genomic sequences revealed that histidine is not present at the position essential for proton currents in either nonmammals or in a prototherian mammal but instead is first observed during the radiation of eutherian mammals (sequences in Table 1). It is retained at this position in eutherians from several superorders, suggesting that this may represent an ancestral form. Furthermore, gene duplication events in primates, including human, have resulted in paralogs that, in one case (TPTE2), remain an active phosphatase while, in another (TPTE), have lost catalytic activity due to sequence changes in the enzyme active site (Walker et al. 2001; Leslie et al. 2007). Yet both human paralogs retain histidine at the essential position in the S4 segment of the voltage sensor and both produce voltage-dependent proton currents in the experimental context studied here. These observations suggest that a selection pressure fixed histidine in this position. However, computational analysis failed to reveal positive selection of this residue (see Materials and Methods: Evolutionary Analysis), suggesting that this is a case of functional adaptation in the absence of sequence-based signals, as has been reported in other systems (Hughes 2008; Yokoyama et al. 2008). The physiological basis of this selection pressure has not been identified but may relate to the requirement for proton currents.

There are two models for the production of proton currents by voltage sensor domains. First is the case of HVCN1, which contains an S1–S4 voltage sensor domain but lacks an identified target domain such as the ion pore of cation channels or the catalytic domain of VSP/TPTE phosphatases (Ramsey et al. 2006; Sasaki et al. 2006). This channel accounts for the endogenous voltage-sensitive proton currents that have been detected in a wide range of eukaryotic cells (Capasso et al. 2011). Proton currents are conducted along an immobilized water wire that penetrates through the sensor domain of HVCN1 but that is absent from Kv channels (Ramsey et al. 2010; Wood et al. 2011). Histidine residues are not present in the S4 segment of HVCN1. In addition, the position corresponding to the histidine that is required for proton currents through chimeric Dr-VSP does not play an essential role in HVCN1 channel activity (Ramsey et al. 2006, 2010). Thus, it is likely that HVCN1 and chimeric Dr-VSP use different mechanisms to conduct protons.

Alternatively, proton currents can be generated through the voltage sensor domain of *Drosophila* Shaker Kv channels following experimental replacement of certain conserved basic residues in the S4 segment with histidine (shown as asterisks, fig. 1*c*). In those mutagenesis experiments, histidine was used to probe voltage-driven conformational changes. The proton currents that resulted are thought to reflect the movement of the introduced histidine from contact with the aqueous environment into the membrane electrical field during voltage-driven sensor activation, and once there to allow this titratable residue to function as a proton shuttle (Starace et al. 1997; Starace and Bezanilla 2001, 2004). Chemical probe studies suggest that the residue in Shaker Kv channels (lysine-380, shown as K-7 in fig. 1*c*) that corresponds to the Hs-TPTE/TPTE2 histidine required for proton currents (histidine-207 in Hs-TPTE, shown as H-9 in fig. 1*c*) may also move from contact with the aqueous environment into the focused electrical field during activation of the sensor domain (Elinder et al. 2001). If similar

Table 1. Sequences of S4 Segment of VSP/TPTE[a]

Species	Protein ID[b]	Sequence
		*
Ascidiacea		
Ciona intestinalis (Sea squirt)	ENSCINP00000021926	LGRLVVLARLLRVVRLARIF**Y**SHQQM
Ciona savignyi (Sea squirt)	ENSCSAVP00000003542	LGRLVALARLIRLVRLGRIL**Y**MHKQA
Cephalaspidomorphi		
Petromyzon marinus (Lamprey)	ENSPMAP00000007388	LPRYNKVLRVLRLIMIIRVW**R**LVSQR
Actinopterygii		
Danio rerio (Zebra fish)	ENSDARP00000074004	IPRVVTFLRSLRILILVRIF**R**LASQK
Gadus morhua (Cod)	ENSGMOP00000001318	DHRGLLFLRILRIIILIRVF**R**LVSQR
Takifugu rubripes (Pufferfish)	ENSTRUP00000027816	IPRAVSFLRFLRIIILVRVF**R**LASQK
Tetraodon nigroviridis (Pufferfish)	ENSTNIP00000012851	IPRAVSFLRFLRIIILVRVF**R**LASQK
Gasterosteus aculeatus (Stickleback)	ENSGACP00000027236	IPRVVTFLRFLRIIILVRVF**R**LAAQR
Oryzias latipes (Medaka)	ENSORLP00000005864	IPRVVNFFRFLRIIILVRVF**R**LAAQK
Aves		
Gallus gallus (Jungle fowl)	ENSGALP00000027464	MPRMVTLLRVLRIVILIRIF**R**LASQK
Meleagris gallopavo (Turkey)	ENSMGAP00000015948	MPRMVTLLRVLRIVILIRIF**R**LASQK
Taeniopygia guttata (Zebra finch)	ENSTGUP00000012387	IPRMVIFLRILRIVILIRVF**R**LASQK
Reptilia		
Anolis carolinensis (Anole)	ENSACAP00000016436	IPRTVILFRILRIIILARVV**R**LASEK
Amphibia		
Xenopus tropicalis (Frog)	ENSXETP00000044740	IPRMVNFLRALRIIILIRIL**R**LASQK
Mammalia		
Prototheria		
Ornithorhynchus anatinus (Platypus)	ENSOANP00000024441	IPRLAILLRPLRIIILIRIF**R**LAVQK
Eutheria		
Bos taurus (Cow)	ENSBTAP00000035646	FPRLRIVLRPVRLVILIRVF**H**LAYQK
Sus scrofa (Pig)	ENSSSCP00000010004	ISKLTFFFRPLRLIILLRVF**H**LVHQK
Equus caballus (Horse)	ENSECAP00000006650	IPRLAIIFRPLRLIILMRVF**H**LAYQK
Canis lupus familiaris (Dog)	ENSCAFP00000008915	IPRLTILFRPLRLIILIRVF**H**LAHQK
Myotis lucifugus (Microbat)	ENSMLUP00000017558	IPRLVILLRSLRLIILMRIF**H**LAYEE
Oryctolagus cuniculus (Rabbit)	ENSOCUP00000015226	IPRLAVLLRPLRLLILVRVF**H**LAYQK
Mus musculus (Mouse)	ENSMUSP00000076435	IPRLAVLLRPLRLLILIRIL**Q**LAHQK
Rattus norvegicus (Rat)	ENSRNOP00000029743	IPRLAVLLRPLRLLILVRIL**Q**LAHQK
Ochotona princeps (Pika)	ENSOPRP00000013347	LAVLFRPLRLIILIRVFHLA**H**QK
Dipodomys ordii (Kangaroo rat)	ENSDORP00000009235	MSRSINLVRPLQLITLLRLL**H**LVNQR
Human		
TPTE (*Homo sapiens*)	ENSP00000355208	IPRWTHLLRLLRLIILLRIF**H**LFHQK
TPTE2 (*Homo sapiens*)	ENSP00000383089	IPRWTHLVRLLRLIILIRIF**H**LLHQK
Pongo abelii (Orangutan)	ENSPPYP00000005901	IPRWTHLVRLLRLIILIRIF**H**LVHQK
Nomascus leucogenys (Gibbon)	ENSNLEP00000016561	IPRWTHLVRLLRLIILIRIF**H**LVHQK
Macaca mulatta (Rhesus macaque)	ENSMMUP00000009683	IPRWTPVVRHLRLIILTRIV**H**LVHQK
Ailuropoda melanoleuca (Panda)	ENSAMEP00000012371	IPRLTILFRPLRLIILIRVF**H**LAHQK
Otolemur garnettii (Bush baby)	ENSOGAP00000020617	IPRWAVFFRTLRLIILIRVF**H**LAPQK
Choloepus hoffmanni (Sloth)	ENSCHOP00000000427	IPRLTILFRSLRLIILLRVF**H**LAYQK
Loxodonta africana (Elephant)	ENSLAFP00000018274	IPRLAVLFRSLRLIILIRIF**H**LAYQK

[a] S4 segment of Hs-TPTE was identified by structural modeling of the solved structures of K^+ and Na^+ channels, and related regions of orthologous proteins were identified using eggNOG 2.0 (see Materials and Methods).

[b] Protein ID identifiers for sequences obtained from Ensembl (http://useast.ensemble.org).

*Site of histidine that corresponds to Hs-TPTE residue 207 and that is responsible for proton current when present in the context of Dr-VSP (yellow shading). Histidine residues in this position are shown in red.

movement also occurs in the voltage sensor of eutherian TPTE/TPTE2, where histidine has been fixed by evolution, then it could permit that residue to conduct protons across the field. Testing this suggestion will require the development of heterologous expression systems that traffic full-length Hs-TPTE/TPTE2 to the cell surface.

Our results suggest that proton currents are conducted by the voltage sensors of Hs-TPTE/TPTE2 and of many eutherian orthologs. However, this current requires strongly positive membrane potentials for activation; it is first observed at $> +20$ mV and full activation requires $> +100$ mV (fig. 2) in the heterologous expression system used here. Mammalian TPTE has been localized in the Golgi complex in spermatogenic cells (Guipponi et al. 2001; Tapparel et al. 2003) and in cell lines following transfection (Guipponi et al. 2001; Walker et al. 2001; Wu, Dowbenko, et al. 2001). But the membrane potential of the Golgi complex is ~0 mV (Schapiro and Grinstein 2000; Wu, Grabe, et al. 2001; Maeda et al. 2008) and may not be sufficient to activate the TPTE/TPTE2 voltage sensor. Similarly, Ci-VSP, which has been reported to be a flagellar plasma membrane protein of *C. intestinalis* sperm (Murata et al. 2005), activates at membrane potentials >0 mV (Sakata et al. 2011), whereas the plasma membrane potential in the sperm of that ascidian is ~−50 mV and may hyperpolarize to ~−100 mV in response to factors released from eggs (Izumi et al. 1999). Finally, *X. laevis* VSP1 and *Xenopus tropicalis* VSP activate at ~0 mV following heterologous

expression, but the membrane potential of those sperm has not been reported (Ratzan et al. 2011). In general then, VSP/TPTE orthologs have functional voltage sensors that have been shown in some cases to regulate catalytic activity (Murata et al. 2005; Hossain et al. 2008; Ratzan et al. 2011), but it is uncertain whether the membrane potential conditions required for phosphatase activation occur under physiological conditions.

It is of course possible that posttranslational modifications occur in vivo that shift the voltage–activation relationship to more negative potentials, as is the case with HVCN1 (DeCoursey 2008). Alternatively, it is useful to recall that the Golgi complex of late spermatogenic cells gives rise to the acrosome (Eddy 2006), an acidic secretory vesicle of sperm (Meizel and Deamer 1978; Lee and Storey 1989; Nakanishi et al. 2001) that plays an essential role in fertilization (Florman and Ducibella 2006). The membrane potential of acidic secretory vesicles in other systems is $>$ +100 mV relative to cytoplasm (Hutton 1982; Loh et al. 1984; Mellman et al. 1986; Breckenridge and Almers 1987). If Hs-TPTE is an acrosomal membrane protein in sperm, then this may provide the specialized conditions for activation of TPTE proton currents. Plausible roles for an acrosomal TPTE may include maintaining the acidic vesicular pH, which is $<$6 when sperm are released from the male epididymis, as well as playing a role in the alkaline shift in acrosomal pH that accompanies sperm capacitation (Meizel and Deamer 1978; Nakanishi et al. 2001).

In summary, we report that a histidine residue is introduced into the cytoplasmic end of the S4 segment of the TPTE voltage sensor during an early stage of the eutherian radiation. This sequence change is fixed in TPTE and paralogs in most eutherian mammals. The presence of histidine at this position permits the voltage sensor domain to conduct voltage-sensitive proton currents.

Supplementary Material

Supplementary figures S1–S3 are available at *Molecular Biology and Evolution* online (http://www.mbe.oxfordjournals.org/).

Acknowledgments

Thanks to William Kobertz, Jose Lemos, and Bayard Storey for comments and advice. This work was funded by the National Institutes of Health grant to H.M.F. (HD062678).

References

Alabi AA, Bahamonde MI, Jung HJ, Kim JI, Swartz KJ. 2007. Portability of paddle motif function and pharmacology in voltage sensors. *Nature* 450:370–375.

Armstrong CM, Bezanilla F. 1973. Currents related to movement of the gating particles of the sodium channels. *Nature* 242:459–461.

Balla T. 2006. Phosphoinositide-derived messengers in endocrine signaling. *J Endocrinol.* 188:135–153.

Bezanilla F. 2008. How membrane proteins sense voltage. *Nat Rev Mol Cell Biol.* 9:323–332.

Breckenridge LJ, Almers W. 1987. Currents through the fusion pore that forms during exocytosis of a secretory vesicle. *Nature* 328:814–817.

Capasso M, DeCoursey TE, Dyer MJ. 2011. pH regulation and beyond: unanticipated functions for the voltage-gated proton channel, HVCN1. *Trends Cell Biol.* 21:20–28.

Chen H, Rossier C, Morris MA, Scott HS, Gos A, Bairoch A, Antonarakis SE. 1999. A testis-specific gene, TPTE, encodes a putative transmembrane tyrosine phosphatase and maps to the pericentromeric region of human chromosomes 21 and 13, and to chromosomes 15, 22, and Y. *Hum Genet.* 105:399–409.

Chetwynd AP, Scott KA, Mokrab Y, Sansom MS. 2008. CGDB: a database of membrane protein/lipid interactions by coarse-grained molecular dynamics simulations. *Mol Membr Biol.* 25:662–669.

DeCoursey TE. 2008. Voltage-gated proton channels: what's next? *J Physiol.* 586:5305–5324.

DeCoursey TE, Cherny VV. 2007. Pharmacology of voltage-gated proton channels. *Curr Pharm Des.* 13:2400–2420.

Eddy EM. 2006. The spermatozoon. In: Neill J, editor. The physiology of reproduction. San Diego (CA): Elsevier. p. 3–54.

Elinder F, Arhem P, Larsson HP. 2001. Localization of the extracellular end of the voltage sensor S4 in a potassium channel. *Biophys J.* 80:1802–1809.

Florman HM, Ducibella T. 2006. Fertilization in mammals. In: Neill JD, editor. Physiology of reproduction. San Diego (CA): Elsevier. p. 55–112.

Guipponi M, Tapparel C, Jousson O, et al. (11 co-authors). 2001. The murine orthologue of the Golgi-localized TPTE protein provides clues to the evolutionary history of the human TPTE gene family. *Hum Genet.* 109:569–575.

Halaszovich CR, Schreiber DN, Oliver D. 2009. Ci-VSP is a depolarization-activated phosphatidylinositol-4,5-bisphosphate and phosphatidylinositol-3,4,5-trisphosphate 5'-phosphatase. *J Biol Chem.* 284:2106–2113.

Hille B. 2001. Ionic channels of excitable membranes. Sunderland (MA): Sinauer Associates Inc.

Hossain MI, Iwasaki H, Okochi Y, Chahine M, Higashijima S, Nagayama K, Okamura Y. 2008. Enzyme domain affects the movement of the voltage sensor in ascidian and zebrafish voltage-sensing phosphatases. *J Biol Chem.* 283:18248–18259.

Hughes AL. 2008. The origin of adaptive phenotypes. *Proc Natl Acad Sci U S A.* 105:13193–13194.

Hutton JC. 1982. The internal pH and membrane potential of the insulin-secretory granule. *Biochem J.* 204:171–178.

Iwasaki H, Murata Y, Kim Y, Hossain MI, Worby CA, Dixon JE, McCormack T, Sasaki T, Okamura Y. 2008. A voltage-sensing phosphatase, Ci-VSP, which shares sequence identity with PTEN, dephosphorylates phosphatidylinositol 4,5-bisphosphate. *Proc Natl Acad Sci U S A.* 105:7970–7975.

Izumi H, Marian T, Inaba K, Oka Y, Morisawa M. 1999. Membrane hyperpolarization by sperm-activating and -attracting factor increases cAMP level and activates sperm motility in the ascidian Ciona intestinalis. *Dev Biol.* 213:246–256.

Jiang Y, Ruta V, Chen J, Lee A, MacKinnon R. 2003. The principle of gating charge movement in a voltage-dependent K+ channel. *Nature* 423:42–48.

Jones S, Zhang X, Parsons DW, et al. (36 co-authors). 2008. Core signaling pathways in human pancreatic cancers revealed by global genomic analyses. *Science* 321:1801–1806.

Krieger E, Darden T, Nabuurs SB, Finkelstein A, Vriend G. 2004. Making optimal use of empirical energy functions: force-field parameterization in crystal space. *Proteins* 57:678–683.

Krieger E, Joo K, Lee J, Lee J, Raman S, Thompson J, Tyka M, Baker D, Karplus K. 2009. Improving physical realism, stereochemistry, and side-chain accuracy in homology modeling: four approaches that performed well in CASP8. *Proteins* 77(Supp l):9:114–122.

Kumanovics A, Levin G, Blount P. 2002. Family ties of gated pores: evolution of the sensor module. *FASEB J.* 16:1623–1629.

Laughlin SB, de Ruyter van Steveninck RR, Anderson JC. 1998. The metabolic cost of neural information. *Nat Neurosci.* 1:36–41.

Lee MA, Storey BT. 1989. Endpoint of first stage of zona pellucida-induced acrosome reaction in mouse spermatozoa characterized by acrosomal H+ and Ca2+ permeability: population and single cell kinetics. *Gamete Res.* 24:303–326.

Leslie NR, Yang X, Downes CP, Weijer CJ. 2007. PtdIns(3,4,5)P(3)-dependent and -independent roles for PTEN in the control of cell migration. *Curr Biol.* 17:115–125.

Loh YP, Tam WW, Russell JT. 1984. Measurement of delta pH and membrane potential in secretory vesicles isolated from bovine pituitary intermediate lobe. *J Biol Chem.* 259:8238–8245.

Long SB, Tao X, Campbell EB, MacKinnon R. 2007. Atomic structure of a voltage-dependent K+ channel in a lipid membrane-like environment. *Nature* 450:376–382.

Maeda Y, Ide T, Koike M, Uchiyama Y, Kinoshita T. 2008. GPHR is a novel anion channel critical for acidification and functions of the Golgi apparatus. *Nat Cell Biol.* 10:1135–1145.

Meizel S, Deamer DW. 1978. The pH of the hamster sperm acrosome. *J Histochem Cytochem.* 26:98–105.

Mellman I, Fuchs R, Helenius A. 1986. Acidification of the endocytic and exocytic pathways. *Annu Rev Biochem.* 55:663–700.

Muller J, Szklarczyk D, Julien P, et al. (11 co-authors). 2010. eggNOG v2.0: extending the evolutionary genealogy of genes with enhanced non-supervised orthologous groups, species and functional annotations. *Nucleic Acids Res.* 38:D190–D195.

Murata Y, Iwasaki H, Sasaki M, Inaba K, Okamura Y. 2005. Phosphoinositide phosphatase activity coupled to an intrinsic voltage sensor. *Nature* 435:1239–1243.

Murata Y, Okamura Y. 2007. Depolarization activates the phosphoinositide phosphatase Ci-VSP, as detected in Xenopus oocytes coexpressing sensors of PIP2. *J Physiol.* 583:875–889.

Nakanishi T, Ikawa M, Yamada S, Toshimori K, Okabe M. 2001. Alkalinization of acrosome measured by GFP as a pH indicator and its relation to sperm capacitation. *Dev Biol.* 237:222–231.

Noda M, Ikeda T, Kayano T, Suzuki H, Takeshima H, Kurasaki M, Takahashi H, Numa S. 1986. Existence of distinct sodium channel messenger RNAs in rat brain. *Nature* 320:188–192.

Ogasawara M, Sasaki M, Nakazawa N, Nishino A, Okamura Y. 2011. Gene expression profile of Ci-VSP in juveniles and adult blood cells of ascidian. *Gene Expr Patterns.* 11:233–238.

Okamura Y. 2007. Biodiversity of voltage sensor domain proteins. *Pflugers Arch.* 454:361–371.

Okamura Y, Murata Y, Iwasaki H. 2009. Voltage-sensing phosphatase: actions and potentials. *J Physiol.* 587:513–520.

Parsons DW, Jones S, Zhang X, et al. (33 co-authors). 2008. An integrated genomic analysis of human glioblastoma multiforme. *Science* 321:1807–1812.

Parsons DW, Li M, Zhang X, et al. (47 co-authors). 2011. The genetic landscape of the childhood cancer medulloblastoma. *Science* 331:435–439.

Payandeh J, Scheuer T, Zheng N, Catterall WA. 2011. The crystal structure of a voltage-gated sodium channel. *Nature* 475:353–358.

Pleasance ED, Cheetham RK, Stephens PJ, et al. (45 co-authors). 2010. A comprehensive catalogue of somatic mutations from a human cancer genome. *Nature* 463:191–196.

Pond SL, Frost SD. 2005. Datamonkey: rapid detection of selective pressure on individual sites of codon alignments. *Bioinformatics* 21:2531–2533.

Pond SL, Frost SD, Muse SV. 2005. HyPhy: hypothesis testing using phylogenies. *Bioinformatics* 21:676–679.

Ramsey IS, Mokrab Y, Carvacho I, Sands ZA, Sansom MS, Clapham DE. 2010. An aqueous H+ permeation pathway in the voltage-gated proton channel Hv1. *Nat Struct Mol Biol.* 17:869–875.

Ramsey IS, Moran MM, Chong JA, Clapham DE. 2006. A voltage-gated proton-selective channel lacking the pore domain. *Nature* 440:1213–1216.

Ratzan WJ, Evsikov AV, Okamura Y, Jaffe LA. 2011. Voltage sensitive phosphoinositide phosphatases of Xenopus: their tissue distribution and voltage dependence. *J Cell Physiol.* 226: 2740–2746.

Ren D, Navarro B, Perez G, Jackson AC, Hsu S, Shi Q, Tully JL, Clapham DE. 2001. A sperm ion channel required for sperm motility and male fertility. *Nature* 413:603–609.

Reymond A, Marigo V, Yaylaoglu MB, et al. (13 co-authors). 2002. Human chromosome 21 gene expression atlas in the mouse. *Nature* 420:582–586.

Sakata S, Hossain MI, Okamura Y. 2011. Coupling of the phosphatase activity of Ci-VSP to its voltage sensor activity over the entire range of voltage sensitivity. *J Physiol.* 589: 2687–2705.

Sasaki M, Takagi M, Okamura Y. 2006. A voltage sensor-domain protein is a voltage-gated proton channel. *Science* 312:589–592.

Schapiro FB, Grinstein S. 2000. Determinants of the pH of the Golgi complex. *J Biol Chem.* 275:21025–21032.

Sjoblom T, Jones S, Wood LD, et al. (29 co-authors). 2006. The consensus coding sequences of human breast and colorectal cancers. *Science* 314:268–274.

Starace DM, Bezanilla F. 2001. Histidine scanning mutagenesis of basic residues of the S4 segment of the Shaker K+ channel. *J Gen Physiol.* 117:469–490.

Starace DM, Bezanilla F. 2004. A proton pore in a potassium channel voltage sensor reveals a focused electric field. *Nature* 427: 548–553.

Starace DM, Stefani E, Bezanilla F. 1997. Voltage-dependent proton transport by the voltage sensor of the Shaker K+ channel. *Neuron* 19:1319–1327.

Suh B-C, Hille B. 2008. PIP2 is a necessary cofactor for ion channel function: how and why? *Annu Rev Biophys Biomol Struct.* 37: 175–195.

Swartz KJ. 2008. Sensing voltage across lipid membranes. *Nature* 456:891–897.

Tao X, Lee A, Limapichat W, Dougherty DA, MacKinnon R. 2010. A gating charge transfer center in voltage sensors. *Science* 328: 67–73.

Tapparel C, Reymond A, Girardet C, Guillou L, Lyle R, Lamon C, Hutter P, Antonarakis SE. 2003. The TPTE gene family: cellular expression, subcellular localization and alternative splicing. *Gene* 323:189–199.

Walker SM, Downes CP, Leslie NR. 2001. TPIP: a novel phosphoinositide 3-phosphatase. *Biochem J.* 360:277–283.

Wang D, King SM, Quill TA, Doolittle LK, Garbers DL. 2003. A new sperm-specific Na(+)/H(+) Exchanger required for sperm motility and fertility. *Nat Cell Biol.* 5:1117–1122.

Wood ML, Schow EV, Freites JA, White SH, Tombola F, Tobias DJ. 2011. Water wires in atomistic models of the Hv1 proton channel. *Biochim Biophys Acta.* 1818:286–293.

Worby CA, Dixon JE. 2005. Phosphoinositide phosphatases: emerging roles as voltage sensors? *Mol Interv.* 5:274–277.

Wu MM, Grabe M, Adams S, Tsien RY, Moore HP, Machen TE. 2001. Mechanisms of pH regulation in the regulated secretory pathway. *J Biol Chem.* 276:33027–33035.

Wu Y, Dowbenko D, Pisabarro MT, Dillard-Telm L, Koeppen H, Lasky LA. 2001. PTEN 2, a Golgi-associated testis-specific homologue of the PTEN tumor suppressor lipid phosphatase. *J Biol Chem.* 276:21745–21753.

Yokoyama S, Tada T, Zhang H, Britt L. 2008. Elucidation of phenotypic adaptations: molecular analyses of dim-light vision proteins in vertebrates. *Proc Natl Acad Sci U S A.* 105: 13480–13485.